Evaluation of machine learning approaches for large scale agricultural drought forecasts to improve monitoring and preparedness in Brazil

Joseph W Gallear[1], Marcelo Valadares Galdos[1], Marcelo Zeri[2], and Andrew Hartley[3]

[1]Rothamsted Research, West common, Harpenden, UK
[2]National Center for Monitoring and Early Warning of Natural Disasters (Cemaden), São José dos Campos, Brazil
[3]Met Office Hadley Centre, FitzRoy Road, Exeter, UK

Correspondence: Joseph W Gallear (joe.gallear@rothamsted.ac.uk)

Abstract. Drought events have increased in frequency and severity in recent years, and result in significant economic losses. Although the Brazilian semi-arid northeast has been historically associated with the impacts of drought, drought is of national concern. From 2011-2019, drought events were recorded in all Brazilian territories. Droughts can have major consequences for agricultural production, which is of particular concern given the importance of soybeans for socio-economic development. Due to its regional heterogeneity, it is important to develop accurate drought forecast and assessment tools for Brazil. We explore machine learning as a method to forecast the vegetation health index (VHI), for large scale monthly drought monitoring across agricultural land in Brazil. Furthermore, we also determine spatio-temporal drivers of VHI across the wide variation in climates, as well as evaluate machine learning performance for ENSO variation and forecasting of the onset of drought stress. We show that machine learning methods such as gradient boosting methods are able to more easily forecast vegetation health in the north and north east Brazil than south Brazil, and perform better during La Niña events than El Niño events. Drought stress which reduces VHI below the commonly used 40% threshold can be forecast across Brazil with similar model performance. SPEI is shown to be a useful indicator of drought stress, with 3 month accumulation periods preferred over 1 and 2 months. Results aim to inform future developments in operational drought monitoring at the National Center for Monitoring and Early Warning of Natural Disasters in Brazil (CEMADEN). Future work should build upon methods discussed here to improve drought forecasts for agricultural drought response and disaster risk reduction.

1 Introduction

Drought events have increased in frequency and severity in recent years and can result in significant economic losses (Cunha et al., 2019; Herweijer and Seager, 2008; Marengo et al., 2017; Brito et al., 2018). According to a 2020 United Nations report, drought has caused at least 124 billion US dollars in economic losses and affected more than 1.5 billion people from 1998 to 2017, furthermore, 5 billion people will live in water scarce areas by 2050 (Brodribb et al., 2020; Wei et al., 2024). Droughts are defined as an extended period in which a water deficit occurs, usually because precipitation is less than average resulting in water scarcity (Cunha et al., 2019). Droughts can have significant consequences for sectors including drinking water supply,

waterborne transportation, electricity production and agriculture (Van Loon, 2015). Agricultural drought can have significant socio-economic impacts because they impact food security. For example, droughts have reduced European cereal yields by 9% on average between 1961 and 2018 (Brás et al., 2021). Sensitivity to drought effects can depend on management factors such as crop selection, irrigation, and tillage practice, as well as climate variability (Wilhelmi and Wilhite, 2002). Agricultural drought has been effectively detected using the vegetation health index (VHI), a proxy for the estimation of vegetation health (Kogan, 2002; Wu et al., 2020). This is because VHI, derived from AVHRR (Advanced very high resolution radiometer) data, responds cumulatively and quickly to changes in vegetation greenness. Therefore the effect of drought can be measured much earlier than that derived from weather data or other drought monitoring tools which allows for faster adaptation responses (Kogan, 2002).

Drought monitoring using vegetation indices such as VHI or NDVI (Normalized difference vegetation index) or VCI (Vegetation condition index) has been developed in several locations using satellite imagery from products such as MODIS, and NOAA STAR (Sadiq et al., 2023; Kloos et al., 2021). VHI is reported to improve on NDVI based monitoring as it provides a measure of vegetation condition relative to long term change (West et al., 2019). Although monitoring past events is useful, a forecasting method would be highly beneficial to provide timely warnings of drought intensification to government officials and other stakeholders. Machine learning has been shown to outperform and hold many advantages over traditional statistical, and time series based prediction methods, in particular machine learning can more easily capture non-linear relationships and does not assume a certain shape of the response function (Leng and Hall, 2020). Machine learning has been used to forecast vegetation indices at timescales including daily, five and seven-day intervals (Kartal et al., 2024; Kladny et al., 2024; Reddy and Prasad, 2018), monthly intervals (Lees et al., 2022), weekly timescales (Barrett et al., 2020), and average vegetation condition values aggregated over 1-3 months (Adede et al., 2019). Models used to predict VHI range from neural networks (Adede et al., 2019; Kladny et al., 2024; Lees et al., 2022; Reddy and Prasad, 2018) to ensemble tree methods such as random forest, and gradient boosting methods (Nay et al., 2018; Tanguy et al., 2023), with some studies using other methods such as gaussian process modelling (Barrett et al., 2020). Results from many such studies show the potential of machine learning and remote sensing indices to effectively forecast agricultural drought. For example, Nay et al. (2018) have used gradient boosting methods to forecast the enhanced vegetation index (EVI) and have demonstrated correlations in agricultural areas between modelled and observed EVI above 0.75. Furthermore, Lees et al. (2022) evaluated forecasts of VCI in Kenya made with neural networks neural networks and deep learning LSTM methods and found excellent performance. This work showed that forecasting VCI one month in advance with an LSTM model can achieve an R^2 value of up to 0.83. Other work has also shown impressive results suggesting great potential for machine learning methods to forecast drought impacts on VHI at large scale.

In Brazil, drought accounts of approximately half of natural disaster related impacts in terms of the number of people affected (Sena et al., 2014). Droughts are of particular concern in the northeast semi-arid region, one of the most densely populated semi-arid regions in the world, which also has the most people living in poverty in Brazil. Nearly 80% of agricultural labour in the northeast is small holder farmers, and rain fed agriculture accounts for 95% of farmed land (Cunha et al., 2019; Marengo et al., 2022). Much work has focused on drought trends in Brazil, with particular focus on the north east semi-arid region (Cunha et al., 2019; Marengo et al., 2017, 2022; Rossato et al., 2017; Zeri et al., 2018). However, in recent years, drought impacts have

affected all regions in Brazil (Cunha et al., 2019; Tomasella et al., 2023). For example, in 2020 drought in Rio Grande do Sul was estimated to have cost R$ 36 billion in losses representing 7.36% of the states GDP (CNA, 2020). Drought has also been linked to inflation, reportedly causing an increase in food prices of 8.03% in 2014 (agência Brasil, 2015). Due to its regional heterogeneity, it is important to develop accurate drought forecast and assessment tools for all of Brazil (Cunha et al., 2019). Drought monitoring and dissemination of drought warnings and intensification in Brazil is undertaken by the National Centre for Monitoring and Early Warning of Natural Disasters (CEMADEN). CEMADEN use several drought indices including the Standardized Precipitation Index (SPI), Root Zone Soil Moisture (RZSM) from remote sensing, and vegetation indices based on remote sensing such as the vegetation health index (VHI). These variables are part of an Integrated Drought Index (IDI), which takes into account classified versions of these products, harmonized to a common spatial resolution and domain. The publicly available IDI index is then used to make the diagnostic of current drought conditions over all regions of the country but is not used to forecast drought metrics. This helps to inform stakeholders of ongoing drought events across the country. In this study, we aim to build on the drought monitoring work at CEMADEN by assessing the potential for machine learning based operational drought impact forecasting at monthly timescales using satellite based VHI observations and drought indices at large scale across Brazil.

In summary, the objectives of this study are:

1. To determine the effectiveness of machine learning methods for VHI forecasts at monthly timescales across agricultural areas of Brazil.
2. To determine which predictors are most useful for drought forecasting models when used across Brazil
3. To determine the effectiveness of machine learning methods for forecasting the onset of VHI drought
4. To determine how ENSO modes of variation affect VHI forecast performance

2 Methods and data

As a scoping exercise for building a drought forecasting machine learning method for Brazil, different methods and indices are evaluated here across different spatial scales across the country. Firstly, various machine learning methods, described in section 2.4, are compared across randomized evaluation years (section 3.2). The best machine learning model from the evaluation is then evaluated against the spatio-temporal variability of the data. Secondly, drought indices described in section 2.2 are compared and evaluated against their correlation with the vegetation health index (section 3.1), model performance, and contribution towards model forecasts (section 3.5). Brazilian agriculture can be significantly affected by changes in the El Niño southern oscillation (ENSO) (Cirino et al., 2015; Júnior et al., 2020). Therefore, model performance against the two modes of the Southern oscillation index is determined. The methods in this study are kept broad to enable others wishing to learn from this work and build their own machine learning forecasting pipelines for other countries and regions at large scales using satellite and remote sensing data products.

Following is a description of the study area of focus for this paper. We use satellite data to enable large scale drought forecasts across major agricultural regions in Brazil. Data was obtained at different spatial and temporal scales, some of which required processing to convert data types to a common spatial and temporal scale. The common spatial scale chosen was 0.25°, with a monthly time step. This was chosen to minimise the amount of spatial up-scaling and down-scaling required.

2.1 Study area

Brazil contains a wide variety of climate conditions and geographic features which present a challenge for prediction when training and evaluating model performance across such a wide area. Spatial variation in climate is particularly significant in Brazil. The climate of Brazil is made up of 9 different Köppen-Geiger climate zones from semi-arid in the northeast, to tropical savanna and tropical rainforest in the northwest, with some areas of marine climate in the South (Peel et al., 2007; Beck et al., 2018). Further to climate zones a wide variety of different biomes are found across the country. Biomes in Brazil have been defined as Amazon, Atlantic Forest, Caatinga, Cerrado, Pampa, and Pantanal (Lopes Ribeiro et al., 2021). The Amazon biome is mainly characterized by rainforest areas and has an equatorial climate with torrential rains distributed throughout the year (Overbeck et al., 2015; Lopes Ribeiro et al., 2021). Atlantic forest is characterized by heavy rainfall due to the proximity to the ocean and winds blowing inward over the continent (Lopes Ribeiro et al., 2021). The Caatinga biome experiences high temperatures and potential evapotranspiration rates that exceed 2500 mm yr^{-1}. This leads to the characterization of the Caatinga as being of low water availability and limited storage capacity of rivers (Lopes Ribeiro et al., 2021). The Cerrado is characterized by large savannahs with a warm tropical subhumid climate and two distinct seasons, wet summers with torrential rains and dry winters (Overbeck et al., 2015; Lopes Ribeiro et al., 2021). The Pampa biome, located in the south, has a wet subtropical climate, and is rainy throughout the year with hot summers and cold winters. Pantanal is made up of poorly drained lowlands which experience flooding from summer to fall months. Precipitation varies from 1000 to 1400 mm yr^{-1} (Ioris et al., 2014; Lopes Ribeiro et al., 2021).

The data was filtered using harvested areas from the crop grids dataset (Tang et al., 2023). The crop grids (Tang et al., 2023) dataset was chosen because it is the newest dataset found with estimates of crop specific growing area for maize and soybean in Brazil. The data was filtered to only contain grid cells which are above the 75^{th} percentile of harvested area across the distribution of harvested area in Brazil. This is to ensure that the grid cells used for training and evaluation are most likely to be indicative of cropland for two major crops grown in Brazil, soybean and maize. Choosing maize and soybean growing areas provides a large spread across different climatic zones of Brazil, and ensures representation of two crops with economic and food security value. Figure 1 shows the spatial distribution of soybean (a) and maize (b) growing areas.

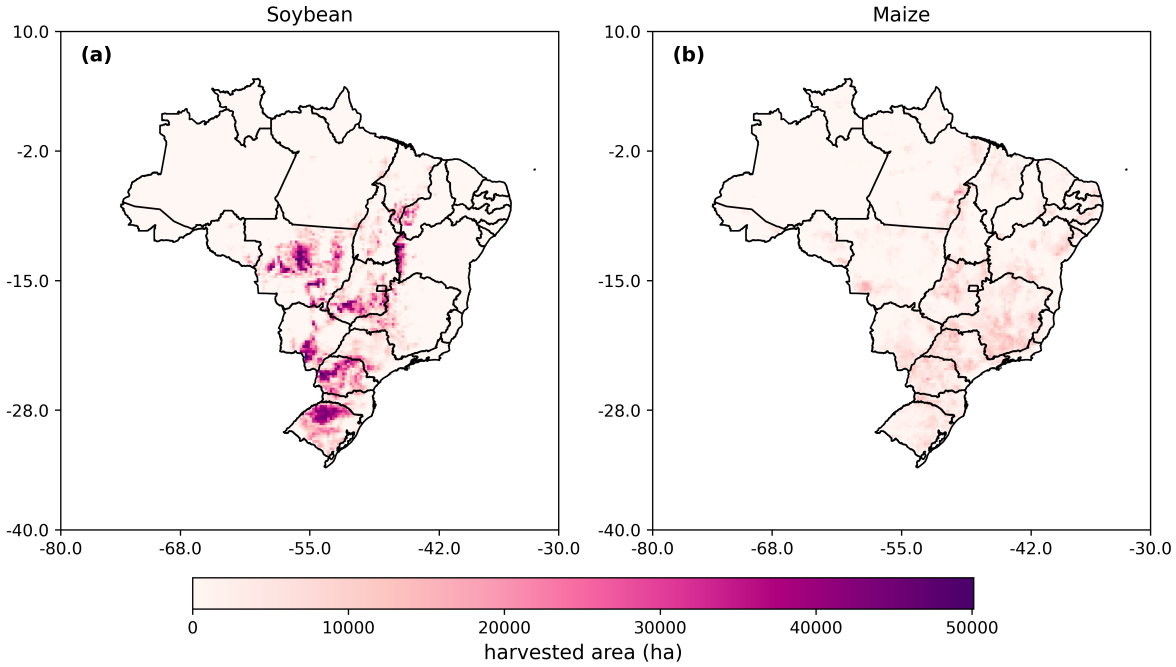

Figure 1. Maps of harvested areas (circa 2020) across Brazil taken from the Crop grids database. Panel (a) shows soybean harvested area. Panel (b) shows maize harvested area.

Using the approach here to select for regions, the cropland area was obtained for a range of locations across Brazil. Much of the most intensely farmed soybean area is in the state of Mato Grosso in central Brazil, as well as Rio Grande do Sul and Paraná in the South and some locations in Bahia in the north east. Maize is a lot less intensely farmed than soybean but just as widespread throughout the country. More maize is grown in Minas Gerais than soybean and is more widespread in the north east of the country.

The large spatial scale of this work makes model training particularly challenging. Agricultural land in Brazil is made up of multiple biomes of differing soil moisture, rainfall, and temperature characteristics (Cunha et al., 2019; Lopes Ribeiro et al., 2021). Meteorological events such as ENSO also affect different parts of the country in different ways. Typically, during El Nino events, there is a reduction in precipitation in the north and northeast regions, while the south experiences higher frequency of heavier rains. In La Nina events, the situation is reversed, with the north and northeast experiencing greater than average rainfall, and south subject to more severe droughts (Cirino et al., 2015).

2.2 Drought Indices

Drought indices were taken from a range of sources, re-sampled to ensure consistent spatial and temporal resolution (see section 2.3) and then assimilated to create a combined dataset to describe drought conditions across Brazil at 0.25° spatial

resolution for each month. To obtain consistent dates across data sources, the dataset ranges from 2003 to 2022. These years also account for seasonal variability and cyclical climate processes, including ENSO which is addressed in this study.

2.2.1 Vegetation Health Index (VHI)

The vegetation health index is a proxy for estimating overall vegetation health, and is expressed in percentage. VHI values below 40% indicate stress conditions. VHI is a composite index which is comprised of the vegetation condition index (VCI) and temperature condition index (TCI). VHI is obtained through the following formula:

$$VHI = \alpha * VCI + (1 - \alpha) * TCI \tag{1}$$

Where α is a coefficient used to determine the relative contribution of TCI and VCI to VHI. The vegetation health index data was obtained from the NOAA STAR satellite based vegetation health system. The NOAA STAR system uses data and products from GOES (Geostationary Operational Environmental Satellite), METEOSAT, MTSAT, and DMSP. Satellite observations are primarily based on radiance measurements taken by the Advance Very High Resolution Radiometer (AVHRR) found on NOAA polar orbiting satellites. The visible and infrared observations are used to determine NDVI as well as TCI, VCI and the vegetation health index (VHI) (Kogan, 1997). VHI data was obtained at the resolution of 0.036° (4km) but then up-scaled to 0.25° to bring to the common spatial resolution of the majority of the input data.

2.2.2 Soil Moisture

Soil moisture is essential to measure the propagation of meteorological drought into agricultural drought and water stress in plants (Zeri et al., 2018, 2022). In this work, soil moisture was obtained from the NASA GRACE satellite (Li et al., 2019). The NASA GRACE satellite data is based on 2 satellites which record changes in the earths gravity field caused by the redistribution of water. Root zone soil moisture was obtained from GRACE for 0.25° grid scale, and a weekly timescale. Temporal resolution was reduced to monthly by averaging soil moisture percentage across 4 week intervals.

2.2.3 Standardized precipitation index (SPI)

The standardized precipitation index (SPI) is a drought index with wide comparability for different locations due to spatially consistent standardization. This makes the SPI a useful index for constructing a model of drought propagation across such a wide spatial domain as agricultural land in Brazil. SPI was first proposed by McKee et al. (1993) to quantify the probability of occurrence of a precipitation deficit at a particular monthly timescale. To determine SPI, precipitation data are fitted to a probability distribution function (usually either gamma or Pearson), before the inverse normal distribution function is used to re-scale probability values, leading to SPI values with a mean of zero and standard deviation of one (Cunha et al., 2019). SPI is calculated over different monthly timescales, Here we use 1,2 and 3 month SPI. Various studies have shown that SPI-3 has the strongest correlation with vegetation response (Sepulcre-Canto et al., 2012) however we also assess 1 and 2 month accumulation periods, which may also be useful for dry environments (Tanguy et al., 2023). SPI indicators with longer accumulation

periods were not tested because such accumulation periods would be longer than the growth periods of maize and soybean. SPI is a widely used index recommended by the world meteorological organisation (WMO). It is also used for operational drought monitoring at CEMADEN (Cunha et al., 2019).

SPI data was taken from the NOAA NIDIS Global precipitation climatology centre (GPCC) (Ziese et al., 2011). We selected SPI data fit to a Gamma distribution. Data was obtained at a 1° resolution then up-sampled using a k-nearest neighbours algorithm to obtain a consistent spatial resolution with the rest of the data set at 0.25°.

2.2.4 Standardized Precipitation-Evapotranspiration Index (SPEI)

SPEI (Standardized Precipitation-Evapotranspiration Index) was first proposed by Vicente-Serrano et al. (2010) as an improved drought index which considers the effect of reference evapotranspiration on drought severity. SPEI is based on the calculation of SPI, however SPEI is determined by computing a climatic water balance (Precipitation - atmospheric evaporative demand), then using this metric to determine probability of a water balance deficit for a given period of time (Beguería et al., 2014). Similar to SPI, a statistical distribution is then used to fit the data, and the data is standardized to produce a mean of zero and standard deviation of one (Beguería et al., 2014).

SPEI data was taken from the global SPEI database (SPEIbase) which was originally at a 0.5° spatial resolution (Beguería et al., 2014). Beguería et al. (2014) use a log logistic distribution to fit the SPEI index. SPEI is an advancement upon the SPI (standardized precipitation index) because the incorporation of evapotranspiration effects accounts for temperature effects on drought which have been shown to significantly affect drought conditions (Rebetez et al., 2006). SPEI values are determined for a number of months, termed accumulation periods. Different accumulation periods could be more useful for specific representations (e.g. longer accumulation periods could be more correlated with longer term storage effects such as groundwater). Here we assess 1-3 month accumulation periods for consistency with SPI accumulation periods and relevance to crop growth periods.

2.2.5 ERA5 Reanalysis predictors

Further data was obtained from the monthly averaged ERA5 database (Hersbach et al., 2019). ERA5 is a reanalysis database which combines models and observations using data assimilation to provide better estimates of meteorological variables at the grid scale (Hersbach et al., 2019). Although ERA5 has an hourly global coverage, we use monthly averaged estimates to allow for consistency with the rest of the data used for this study.

From this resource, 2 metre temperature, potential evaporation, and surface thermal (longwave) radiation downward were obtained. Temperature variables are important to capture drought effects brought on by high temperatures rather than solely a deficit in rainfall. This can be especially important for flash drought events, which are typically caused by compounding effects of rainfall deficits and high temperatures which increase evaporative stress (Christian et al., 2021).

2.2.6 Total monthly precipitation

Precipitation data was obtained from the Climate Hazards Group Infrared Precipitation with Station data (CHIRPS) database (Funk et al., 2015). CHIRPS is a quasi-global database (ranging from 50°N - 50°S) which is available at multiple spatial resolutions including 0.25°. The CHIRPS dataset combines satellite data with *in situ* measurements to provide a gridded dataset of appropriate spatial extent for this study. CHIRPS has been validated against other datasets and *in situ* observations and has been used for similar studies in other regions (Lees et al., 2022). Total monthly precipitation is included as a variable to provide a benchmark comparison to precipitation indices when analysing feature importance.

2.3 Data Processing and Sampling Methods

Data was originally obtained at a range of different spatial and temporal resolutions. Table 1 shows the original resolution of each of the indices used. Where spatial resolution has been decreased (spatial down sampling) this is done through averaging. Where spatial resolution has increased (spatial up sampling) this is calculated using a k-nearest neighbours algorithm. All data was spatially corrected to a 0.25° spatial resolution. Some data was obtained at weekly or daily timescales, in this case, data was averaged per month for each grid cell location to obtain average monthly estimates of each variable.

Table 1.

Variables considered for use in this study with original spatial (degrees) and temporal resolution, source, and abbreviation used in this paper.

Predictor	Spatial resolution	Temporal resolution	Source	Abbreviation
2 Metre temperature	0.25	Monthly	ERA 5	t2m
Potential evaporation	0.25	Monthly	ERA 5	pev
Surface thermal radiation downwards	0.25	Monthly	ERA 5	longrad
Root zone soil moisture	0.25	Weekly	NASA GRACE	RZSM
Total precipitation	0.25	Daily	CHIRPS	precip
Vegetation health index	0.036	Monthly	NOAA STAR	VHI
SPEI 1	0.50	Monthly	LCSC	SPEI1
SPEI 2	0.50	Monthly	LCSC	SPEI2
SPEI 3	0.50	Monthly	LCSC	SPEI3
SPI 1	1.00	Monthly	GPCC	SPI1
SPI 2	1.00	Monthly	GPCC	SPI2
SPI 3	1.00	Monthly	GPCC	SPI3

2.4 Forecasting Methods

We evaluate a range of machine learning methods for the forecasting of vegetation health index 1 month in advance before using the best model to assess the performance of further forecasts aimed at predicting vegetation health index 2 and 3 months in advance and more closely analysing spatio-temporal model performance. Methods here compared are Random Forest (Breiman, 2001), gradient boosting (Friedman, 2001), artificial neural networks (LeCun et al., 2015) k-nearest neighbours regression, ridge regression and a multiple linear regression for comparison.

Random forest and gradient boosting are tree based methods which construct an ensemble of decision trees. Decision trees partition data into subsets based on conditions at each leaf node of the tree. Tree depth and complexity can be specified by the user. random forest constructs a specified number of trees and then averages the result of each individual tree. Different trees are trained on different randomized sub samples of the dataset, a method known as bootstrapping. Gradient boosting methods differ from random forest in that decision trees are trained sequentially rather than simultaneously, with residual error from previous decision trees used to improve each subsequent model.

Artificial neural networks are layered networks of inter connected units which each contain a set of weights. Weights are optimized against an error term and the training data using a separate optimization algorithm. Deep neural networks are those which contain many subsequent processing layers (LeCun et al., 2015). Neural networks are flexible architectures, with many adaptations being constructed for different tasks. Here, we compare a fully connected neural network. Fully connected neural networks are named as such because each node in the preceding layer is connected to each node in the subsequent layer.

K-nearest neighbours regression is a semi-supervised learning method which uses a user defined k value to learn the k-nearest data based on a distance calculation. Most commonly this method uses the euclidean distance metric for this approach, however other distance metrics may be used (Chomboon et al., 2015). Multiple linear regression and ridge regression are used as linear comparisons to more complex methods used here to assess the appropriate level of complexity for the model required.

A comparison is also made between each of the above described models and a seasonal average model (denoted SEA AV). The seasonal average model is simply the average value of VHI for a particular location and month. The purpose of this model is to provide a low benchmark comparison to assess model performance relative to that which would be achieved by simply using the seasonality of VHI alone.

2.5 Cross validation and training procedure

We cross validated models across a large span of years to provide a general picture of model performance regardless of evaluation period. Evaluation was split by year to avoid the influence of spatial autocorrelation on data leakage between training, validation and testing splits. Model evaluation metrics were obtained by training 10 separate models with the same set of hyperparameters each tested using a randomized hold out test year. Results for each model are then aggregated to produce metrics across the 10 year aggregation period. Further to this, we also evaluated optimal hyperparameter values, the results of which can be found in appendix 6. To optimize hyperparameters, the data was again split by year to avoid any shared information between splits, however data was also split 3 times into training, validation and testing. For this method, we used

a hold out evaluation data set of 5 random years. These years were chosen as 2006, 2011, 2016, and 2019. The rest of the data is split between 2 randomized folds based on year. The best set of hyperparameters across both folds are used to train each model before subsequent testing on the evaluation dataset. The decision was made to train and evaluate on as much data as possible here with sub-optimal parameters to provide the best indication of general model performance across a wider range of evaluation years. This allows us to better look into effects of ENSO on model performance and inter-annual variability regardless of specific hyperparameter optimization. Although hyperparameter optimization did change the results of individual models slightly, the best model was the same across both training and evaluation procedures. Furthermore, it was found that the best model results were achieved by simply training on more data, rather than a specific set of hyperparameters.

2.6 model evaluation methods

Model performance is evaluated using complementary mean absolute error and coefficient of determination metrics (R^2). Coefficient of determination is used to determine the performance of the model against a wide degree of variability, with high coefficient of determination indicating that the model captures both extremes at the low and high end of the distribution.

2.6.1 Drought onset forecasting evaluation

Furthermore, prediction of the onset of drought impact is evaluated in section 3.4. Here, we use precision and recall as metrics for evaluating whether the model correctly predicts when VHI decreases below 40%. The 40% threshold is chosen because it is used in many drought monitoring systems as the critical threshold at which warnings are issued (Kogan, 1997; Kogan et al., 2013; Gidey et al., 2018). Recall and precision are defined by the four classification metrics used to determine classification performance. True positives (TPs), True negatives (TN), False positives (FP), and False negatives (FN). A true positive is determined when the observed value of VHI falls below 40% and the model correctly forecasts a value of VHI below 40% for that month. Conversely, if the observed value of VHI falls below 40% but the model forecasts a value above 40% this is a false negative. Likewise, if the model forecasts a value below 40% which was not observed, this is classed as a false positive. Finally, if both the observed and predicted values fall above the 40% threshold a true negative is determined. Table 2 defines each of the classification values.

Table 2.

Definitions of classification metrics used to determine model performance for accurately predicting the onset of drought impacts on VHI.

classification	observed value (%)	forecast value (%)
True positives (TP)	$VHI < 40$	$VHI < 40$
False positives (FP)	$VHI > 40$	$VHI < 40$
False negatives (FN)	$VHI < 40$	$VHI > 40$
True negatives (TN)	$VHI > 40$	$VHI > 40$

Recall and precision are defined using the classification determined in Table 2. Recall is a measure of the number of true positives as a ratio of the number of true positives plus the number of false negatives. Formally, recall is defined as:

$$recall = \frac{TP}{TP + FN} \tag{2}$$

In this manner, recall can be thought of as the performance of the model in proportion to the bias towards predicting the negative class (values above 40%). Precision is similarly defined as:

$$Precision = \frac{TP}{TP + FP} \tag{3}$$

Precision is therefore defined as the number of true positives as a ratio of the number of true positives plus the number of false positives. It can therefore be thought of as the performance of the model in proportion to the bias towards predicting the positive class (values below 40%).

3 Results

The results of this paper aim to present a first look at the potential of machine learning to produce monthly VHI forecasts and the impacts of drought on VHI across Brazil. Model performance indicates great benefit can be obtained from forecasting sub-seasonal vegetation health 1 month in advance. Forecasts further in advance, for 2 and 3 months may also be achievable but show much greater model uncertainty with methods tested.

3.1 Drivers of VHI variability

Figure 2 shows the correlations between SPI and SPEI with vegetation health index of the following month. Longer accumulation periods lead to greater correlations with VHI. SPEI values are more strongly correlated with VHI values in some regions than SPI. Regions where this occurs include northern Mato Grosso in central Brazil, and the south. Neither SPEI or SPI have very strong correlations with next months VHI in these regions, but SPEI typically has correlations which are less weak.

Other variables included in the modelling process may also be significant drivers of VHI. Figure 2 shows the correlations between Next month's VHI and Root zone soil moisture (RZSM), precipitation, potential evaporation, downward longwave radiation, 2 metre temperature and VHI of the present month. As expected, the highest correlations are between the present and subsequent months VHI. RZSM has high correlations in the north east although very weak correlations around central Brazil. 2 metre temperature generally has greater correlations with next months VHI than downward longwave radiation.

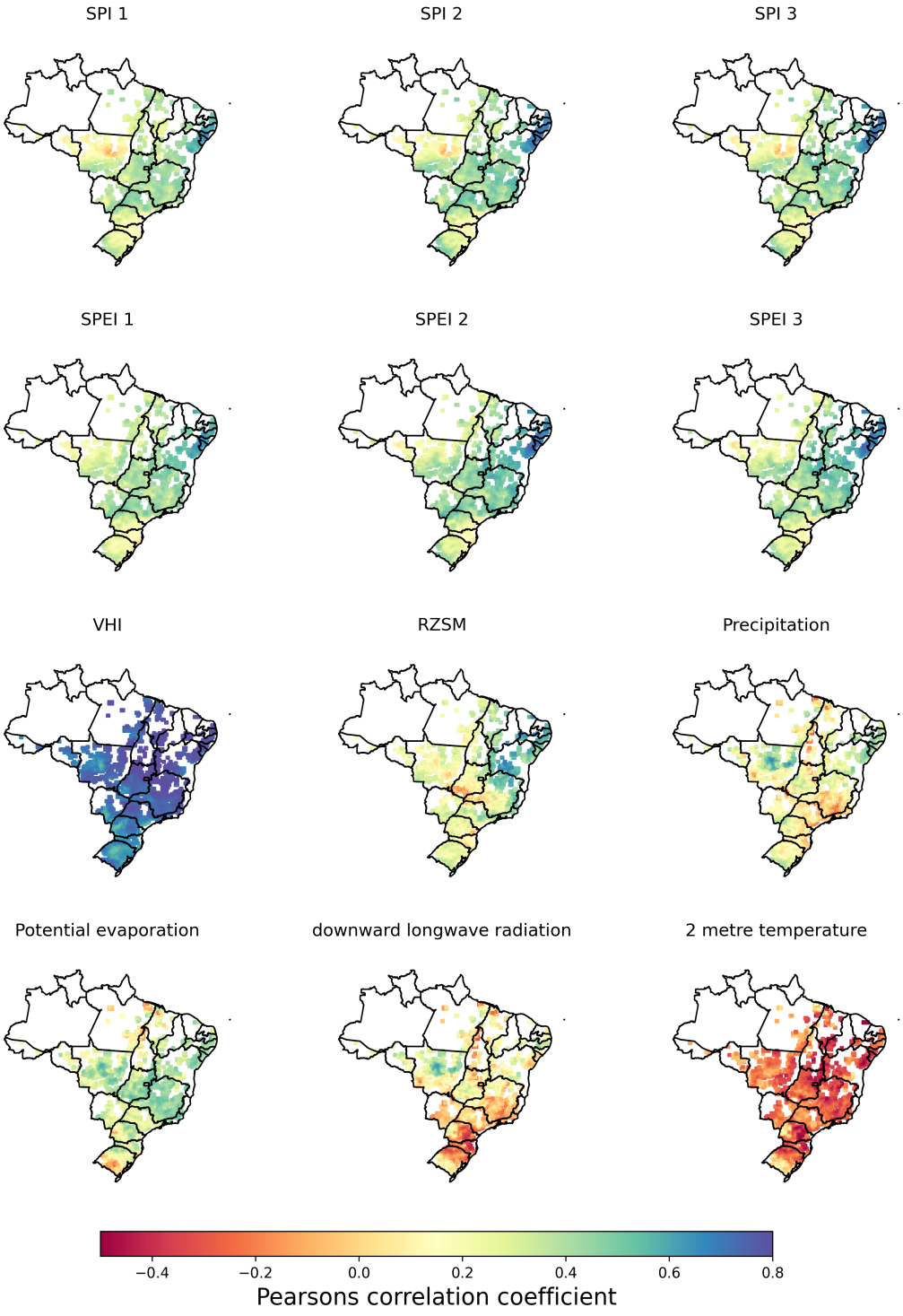

Figure 2. Correlation coefficient between the vegetation health index and predictor variables used in this study.

The correlations in Figures 2 were used to inform 1 month forecasts of VHI using a variety of machine learning methods presented in the subsequent section.

3.2 VHI forecasts

The initial selection of models described in section 2.4 are compared here in Figure 3. Gradient boosting model (GBM) was able to achieve greater performance across randomized test years than the other models. For this reason, the GBM model was then chosen for further analysis including testing against later years. Feature importance is described in section 3.5. SEA AV denotes a 'seasonal average' benchmark, which is simply a model which predicts each month at each location as the historical average for the month, for the location to be predicted. All models outperform this low benchmark. This allows for the conclusion that all models obtain performance greater than that which can be inferred entirely from seasonal variability in VHI.

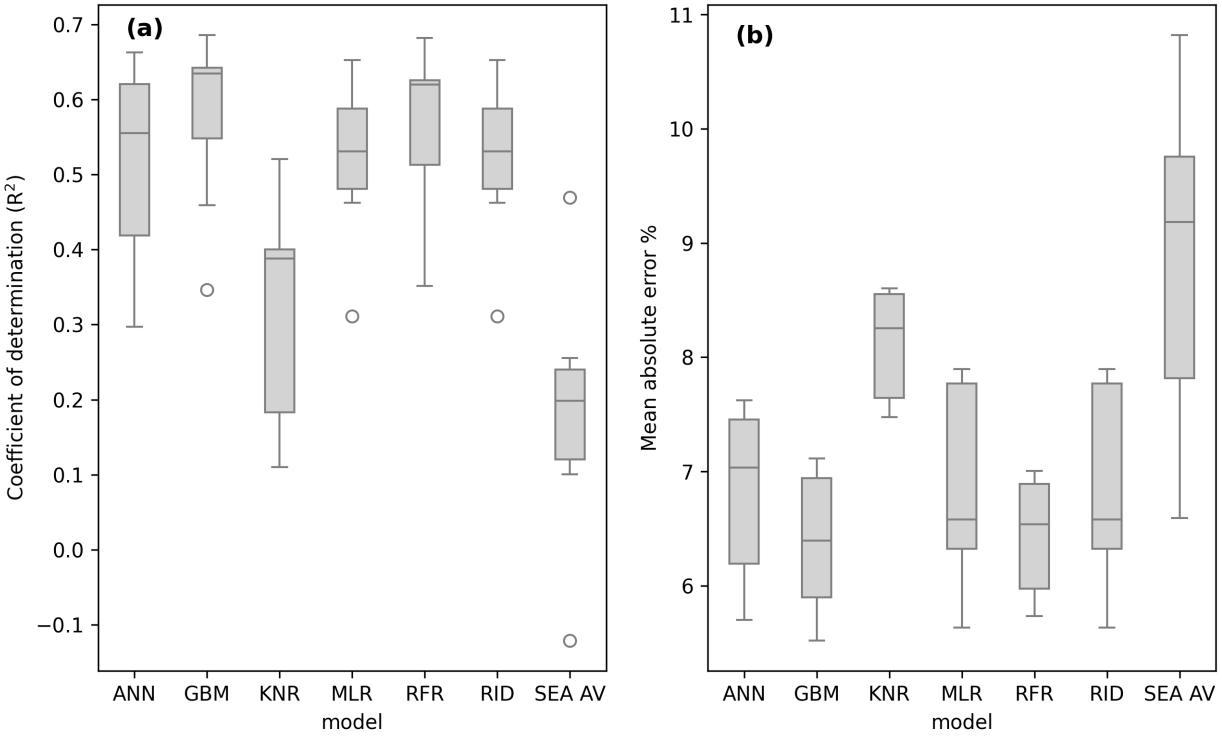

Figure 3. VHI forecasting model performance (a: coefficient of determination, b: mean absolute error) across a range of initially selected models. SEA AV refers to the monthly average model.

The best model from the initial comparison (GBM model) was taken and further assessed across the spatial domain (Figure 4) and for the mode of the southern oscillation index (SOI) (Figure 5). Model performance in terms of R^2 is greatest in the east, some of the weakest correlations are in the west of the country, south and central regions. Panel (c) of Figure 4 shows that generally R^2 values are between 0.6 and 0.75 for the gradient boosting machine learning method across grid cells. The distribution of mean absolute error values is less skewed, with most falling between 5-6%.

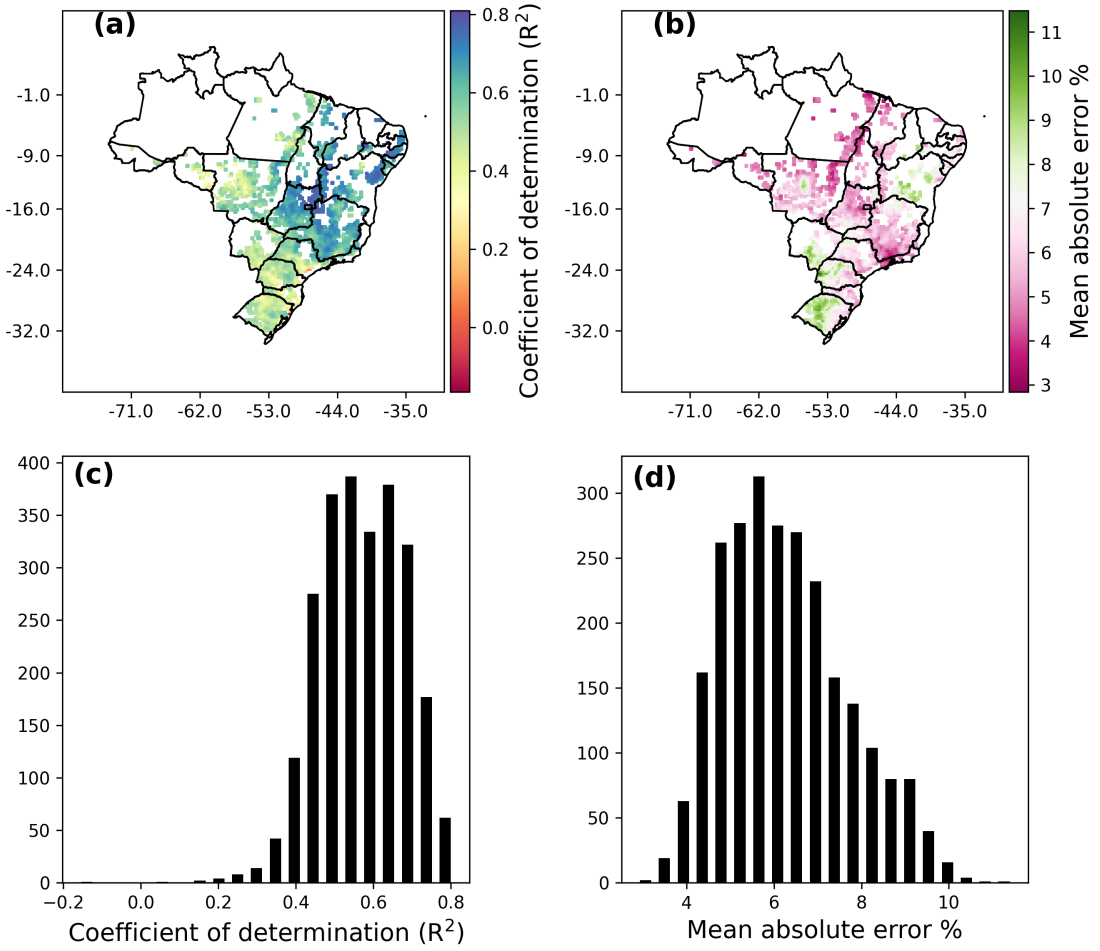

Figure 4. VHI forecasting model performance for the best model (GBM) across the spatial domain in Brazil, showing the R^2 score and mean absolute error for each grid cell location. Panels (a) and (b) show the spatial distribution of model performance for the two metrics, panels (c) and (d) show histograms of model performance metrics.

3.3 Effects of Southern oscillation index

Here, model performance metrics are split into El Niño and La Niña evaluation periods. Figure 5 shows how spatial trends in model performance can be affected by ENSO. For El Niño periods, model R^2 significantly reduces for central Mato Grosso, and there is a broader trend of decreases in model R^2 values across the South. This trend is also shown for mean absolute error. Generally, La Niña periods are forecast better than El Niño periods.

Figure 5 also shows how the effects of the ENSO can lead to either under or over-prediction of VHI depending on location and ENSO mode. of note is the over-prediction of VHI in central Mato Grosso in El Niño periods and underprediction in the south. Generally, model performance is less affected by La Niña than El Niño.

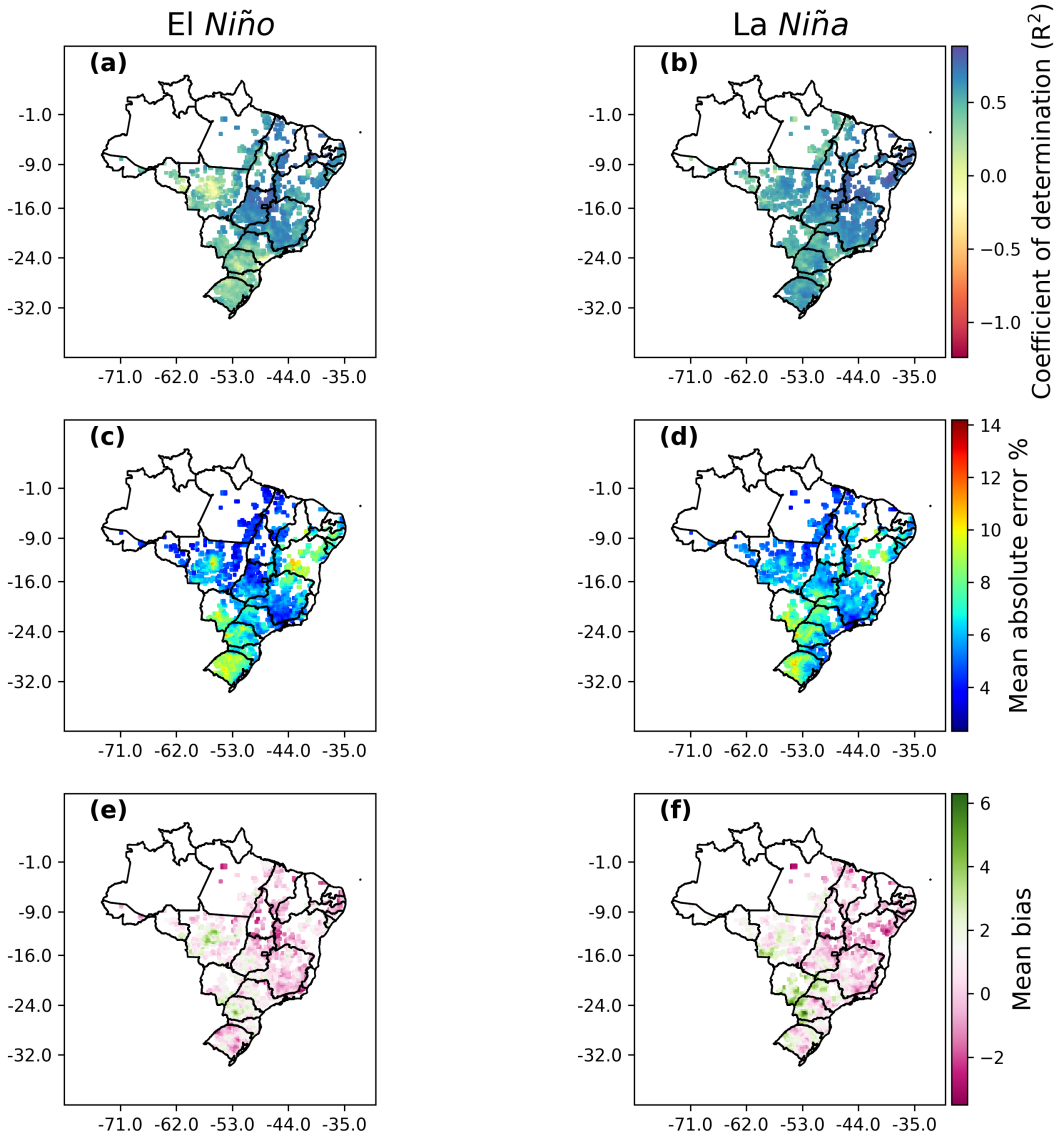

Figure 5. VHI forecasting model performance against Positive and negative modes of the southern oscillation index, negative SOI is associated with El Niño, and positive SOI is associated with La Niña weather events. Metrics are coefficient of determination (panels a and b), mean absolute error (c and d) and mean bias (e and f).

3.4 Predicting onset of drought impacts on VHI

It is also important for models to be able to forecast when drought impact may reduce VHI below the alert threshold of 40%. The metrics described in section 2.6 are used here to determine the performance of the best model for forecasting if VHI may fall below 40% in the following month. Typically, model precision is greater than recall, meaning that there is a bias towards over prediction of values above 40% rather than over-prediction of values below 40%. This is to be expected given the distribution of VHI values results in more values above this value.

Figure 6 shows overall recall and precision (a) and when separated to El Niño (a) and La Niña weather (b) weather events. The El Niño affects model performance by increasing the range of precision and recall values, increasing the number of those values at the low end of the range of values.

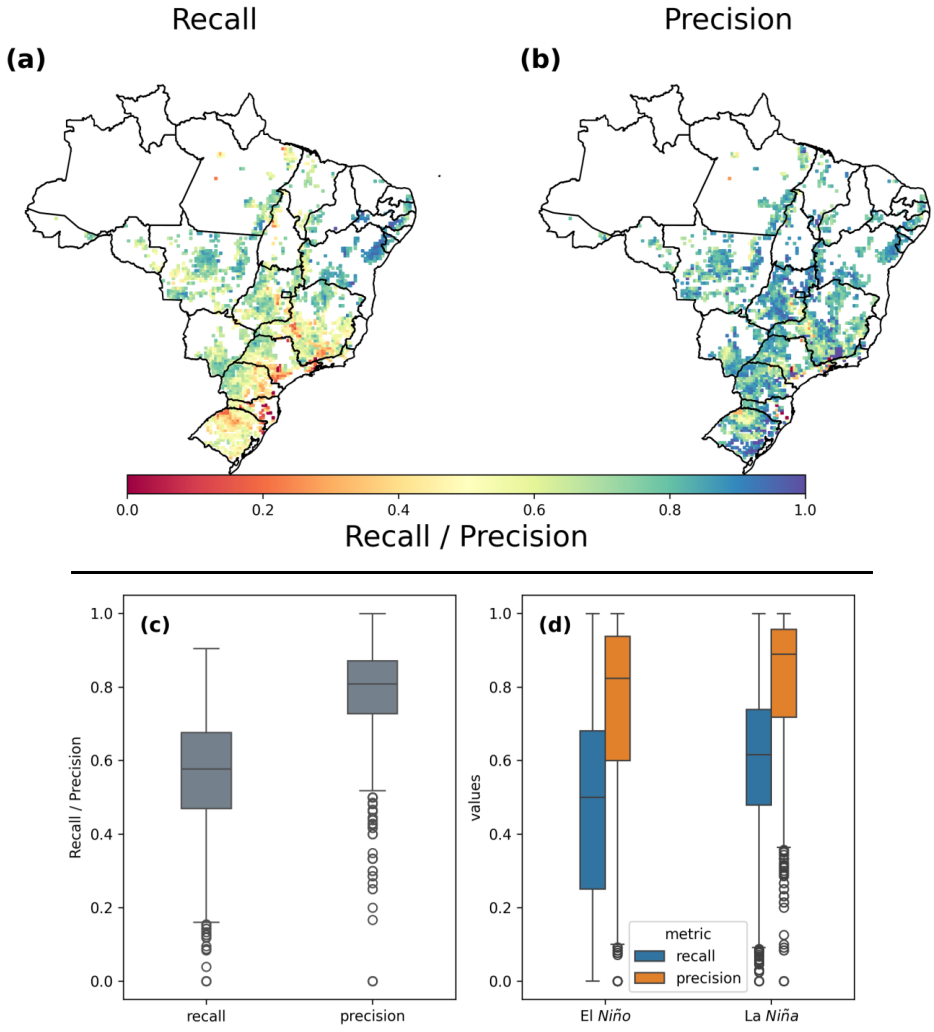

Figure 6. Recall and precision metrics shown both spatially (a) and (b) and as boxplots (c) and (d), panel (d) also shows the effects of ENSO on recall and precision.

Figure 6 also shows the spatial pattern of recall and precision (section (i)). Generally, recall is lower than precision although there is no clear spatial trend in which regions may have higher or lower recall or precision. Lowest recall tends to be in coastal areas.

3.5 Feature importance

320 Correlations are measured between the strength of correlation between input and output variables and their correlation with model performance. This is shown for SPI and SPEI indices in Figure 7 and for temperature and VHI in Figure 8. Here we

show the relationship between the strength of correlation between input variables and observed VHI, and model performance measured by coefficient of determination.

Figure 7 shows that model performance is more highly correlated with longer accumulation periods of SPI and SPEI. Furthermore, SPEI likely has a greater effect on model performance than SPI. Figure 8 indicates that 2 metre temperature may be a stronger variable to use to capture the effects of temperature on VHI than other similar but correlated variables such as incoming longwave radiation and potential evaporation.

Spearman-rank Correlations between predictors are found in section 8. This was determined to show how correlations may affect feature importance and the highest correlating features with VHI.

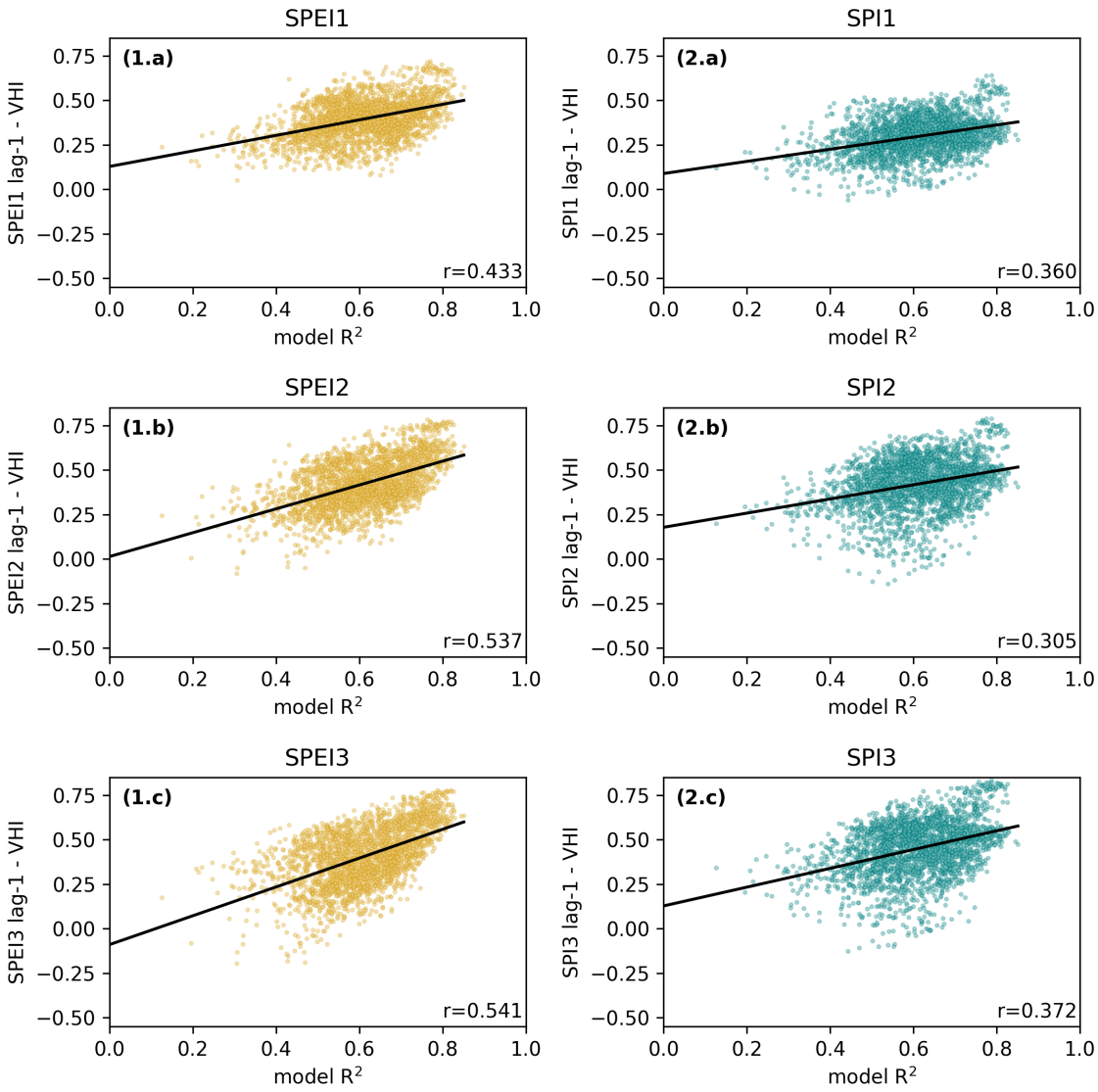

Figure 7. Pearson correlation coefficient between indices SPEI and SPI (1-3) and VHI against model prediction performance measured by coefficient of determination (R^2). A line of best fit is plotted in blue for each panel with R value in the bottom right. Each point represents the modelled R^2 at a single grid cell with corresponding SPEI/SPI and VHI relationship.

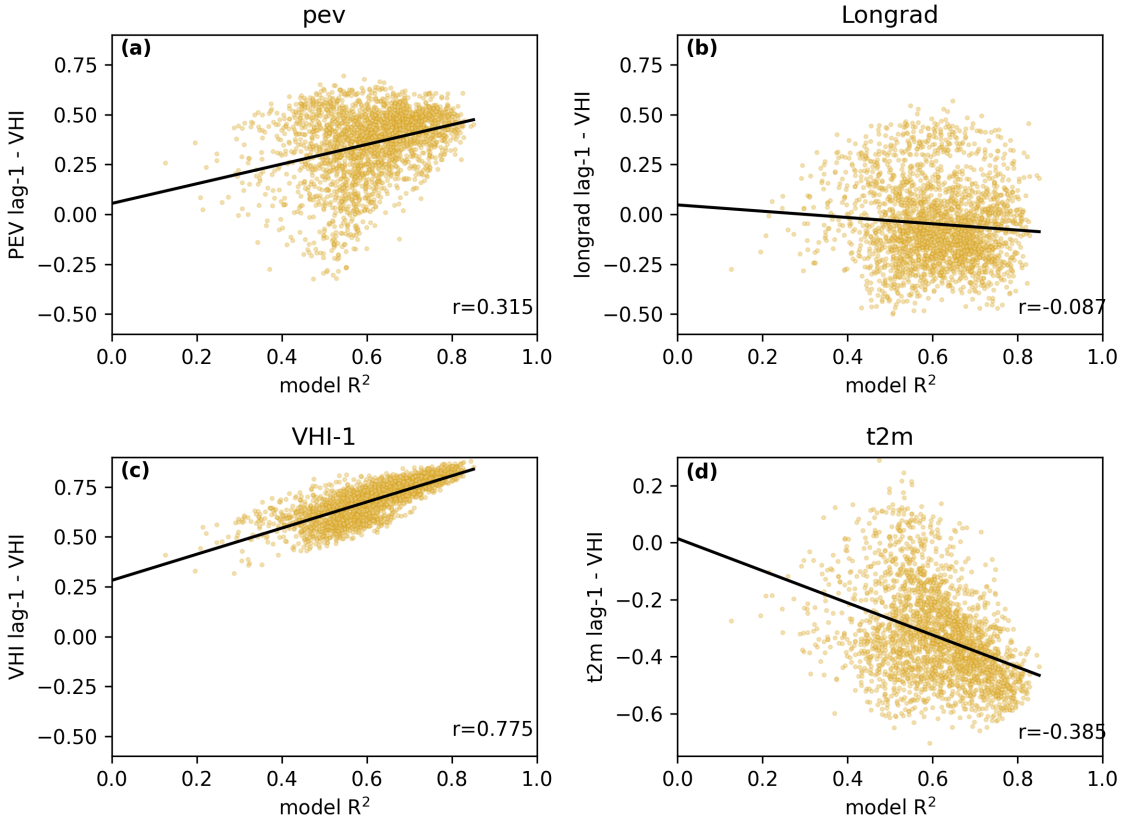

Figure 8. Pearson correlation coefficient between temperature effects and VHI against model prediction performance measured by coefficient of determination (R^2) as well as VHI autocorrelation. A line of best fit is plotted in blue for each panel with R value in the bottom right. Each point represents the modelled R^2 at a single grid cell with corresponding variable and VHI relationship.

4 Discussion

Model performance varies upon the relationship between soil moisture, SPEI, SPI and VHI across Brazil, as well as the temporal autocorrelation of VHI. VHI in Southern Brazil (where rainfall is generally higher) is generally more difficult to forecast. For this reason, forecasting models presented here are most appropriate to be used in primarily moisture driven regions (with most useful results for the north east). The results presented here are of great significance for drought monitoring and forecasting efforts in Brazil and for others who may use studies such as this to inform other drought monitoring and forecasting work for other countries and regions. Here we show that machine learning is capable of accurately forecasting the spatio-temporal variability in VHI across Brazil, and can also determine when VHI values are likely to fall below the 40% drought stress threshold. Gradient boosting methods are an excellent method to use for both these evaluation metrics. Model performance is affected by El Niño events in the south and central Mato Grosso. Although machine learning is able to forecast

when VHI will fall below 40%, typically, model precision is greater than recall. This means that the model is more biased towards forecasting VHI values above 40% which is as expected given the distribution of VHI values.

4.1 Regional variability in VHI

Vegetation health index variability is greatest in the northeast semi-arid region of Brazil. In this region, VHI is more greatly driven by rainfall and subsequent moisture effects than any other region in Brazil. This makes the northeast the most easily forecast region. In The south and mid-west region (particularly Mato Grosso State) This trend results in poorer model performance in these regions. Subsequently, temperature effects are greater drivers of VHI in these regions. This is likely due to the regional effects of limiting factors, which limit the growth of crops and vegetation and are known to vary spatially with varying climate (Sacks et al., 2010).

4.2 Spatial heterogeneity and temporal autocorrelations

Temporal autocorrelations across space indicate high monthly autocorrelation for VHI. These temporal autocorrelations help to improve the ability to forecast VHI on monthly timescales. VHI temporal autocorrelation is highest in the northeast, This is a decisive factor contributing to greater model performance in this region.

4.3 How to build the most useful model for sub-seasonal VHI forecasting in Brazil

The results presented here provide key insight into the development of machine learning methods to forecast the effects of drought on vegetation health. Recommendations for how to build a forecasting model come in the form of two key factors: ML architectures and indices. Accurate forecasting requires a method of appropriate complexity. The appropriate level of complexity should strike a balance between model explanatory power and number of parameters to constrain. This study clearly indicates that linear methods such as multiple linear regression lack the explanatory power to effectively forecast forthcoming drought impacts and trends in VHI. Conversely, some methods may be too complex, in this circumstance, gradient boosting methods outperformed the artificial neural network. Neural networks contain a large number of parameters, which ultimately require more data to be adequately constrained, this can cause model training to be of far greater challenge.

Choice of climate indices and variables are also a key question when building a forecasting model. In Brazil, the wide range of biomes across the country can mean that the influence of certain indices such as SPEI and SPI may be of greater importance in some regions than others. Particularly, dry areas in the north east which are more effected by drought based indicators SPEI, SPI and RZSM. Furthermore, although SPEI may be more influential than SPI, it is more important that longer term indicators of 3 months are used above shorter 1 month accumulation periods. Of course, using the temporal autocorrelation in VHI is a key factor in determining model performance. Regions which have the greatest monthly VHI autocorrelation also are the most easily forecast. Temperature variables are more useful for the forecasting of VHI in south Brazil, where typically rainfall is higher and drought is less common in occurrence.

Here models were trained for VHI value forecasting and then the ability of the best model to determine onset of drought is found in section 3.4. This resulted in high precision with slightly lower recall, meaning that model bias is towards forecasting values of VHI above the 40% threshold. For the forecasting of drought onsets, a more effective method to train models may be to use a classification model with altered training data to over-sample VHI instances in which VHI is below 40%. There are many methods which can be used to improve data set balance and improve recall, such as ensemble based methods, over and under-sampling strategies, and synthetic minority oversampling methods (Chawla, 2010). However, in doing this, forecasting of VHI values would require a separate model.

4.4 Scope of methods analysed

Here we analyse machine learning methods including artificial neural networks, gradient boosting and random forest methods, nearest neighbour methods and linear regression methods. Among methods excluded include convolutional LSTM models as discussed by Kladny et al. (2024) as well as other deep learning methods such as an ensemble of temporal convolutional neural networks (Miller et al., 2023). These model frameworks were excluded from the methodology following the general principal of Occam's razor to evaluate simpler methods first before expanding the scope of the work to more complex methods with greater numbers of parameters given time constraints. Evaluating such methods in the region should be a priority for future work building from this study.

In this study, machine learning methods are trained and evaluated on both maize and soybean growing area together. No results are presented for models trained on maize and soybean growing area separately. Some preliminary exploratory analysis indicated that the differences between the performance of models trained on maize and soybean growing areas separately would not be significant. A likely contributing factor to this is that there is much overlap between maize and soybean growing areas (see Figure 1), particularly because maize is often grown in rotation with soybean (dos Santos Canalli et al., 2020; Carvalho et al., 2014).

4.5 Future model developments for Brazil drought monitoring

To expand on the scope of this study, further work should focus on the application and assessment of machine learning architectures such as those described in the previous section (4.4). Such methods have been shown to improve vegetation health forecasts in other regions (Kladny et al., 2024; Miller et al., 2023) and so may also improve results here. Furthermore, improvements could be made to the forecasts of specific months key for agricultural production. Here, the best model trained can have variable performance depending on month of assessment. A greater assessment of sampling methods or the targeted use of model ensembles may improve the stability of model performance for key months. For many regions November - March of the next year can encompass a typical growing season (CONAB, 2022). Therefore, these months are of greater importance.

This work aims to inform future developments in drought monitoring for Brazilian agriculture at CEMADEN. Forecasting VHI would help to identify areas potentially affected by drought one month in the future. Currently, forecasting of next month's SPI is used to measure the potential impacts of drought, since rainfall anomalies are critical as a hazard. The forecast of VHI can bring information on potential impacts, since it reflects on the vegetation health. This information is essential for disaster

preparedness and planning of future actions to support areas affected by drought. The identification of drought evolution can inform decision makers in several agencies and levels of government on how to manage resources destined to alleviate drought impacts on agricultural activities.

5 Conclusions

This study addresses several questions important for building an agricultural drought forecasting framework for Brazil. In summary, the key conclusions of this work are as follows. Machine learning methods have great potential to be used to forecast agricultural drought 1 month in advance, and gradient boosting methods are able to achieve up to 0.8 coefficient of determination in some areas such as the northeast, making them an especially promising method to use. This work also shows that for some regions across Brazil SPEI may be a more useful indicator than SPI alone. For the agricultural drought onset forecasts, models also performed well but further work is needed to test different methods of classification. ENSO variation had small effects on model performance, with El Niño effects being more difficult to predict than La Niña effects.

These findings are of significance for future drought monitoring and forecasting work in Brazil as well as for other regions in which drought monitoring and forecasting systems using machine learning are being considered or developed. Specifically, in showing how machine learning methods perform across Brazil, this research provides a first benchmark set of results for agricultural drought forecasts in the country. This also provides useful information about the spatio-temporal pattern of model performance. For future research outside of Brazil, this work provides a case study as to how machine learning methods perform across a wide area with large diversity in climate.

Future work should aim to build upon these results to further aid drought monitoring efforts with improvements to model performance through additional pre-processing techniques and further assessment of machine learning modelling frameworks.

6 Appendix A

Here we show results from the optimization of certain hyperparameters for the models investigated in this work. Hyperparameters are global parameters which affect the learning process rather than the model itself. Hyperparameters can include the learning rate of a neural network, the number of neighbours to use in the k-nearest neighbours algorithm, or the number of decision tree estimators present within a random forest model or gradient boosting machine. We undertook minimal hyperparameter optimization. We use the coefficient of determination to optimize hyperparameters across cross validation folds. For gradient boosting and random forest models, we optimize the number of estimators which comprise the model. We found that above a certain threshold value (typically 2-10) the number of estimators which achieved the best results can vary if repeating optimization. For the K-nearest neighbors algorithm, the number of neighbors was varied between 5 and 1000, 500 neighbors was found as the optimum value. For Ridge regression, the regularization parameter, (α) was optimized however results did not improve above those of the default value (1). The neural network was optimized by varying the number of neurons in each hidden layer, and the number of epochs, which is the number of iterations through the dataset when training. Through

optimization we determined 30 epochs with 25 neurons in each layer. We kept the number of hidden layers as small as possible (1 layer) to avoid over-parameterization. Model results with these optimized parameters are found in Figure 1a.

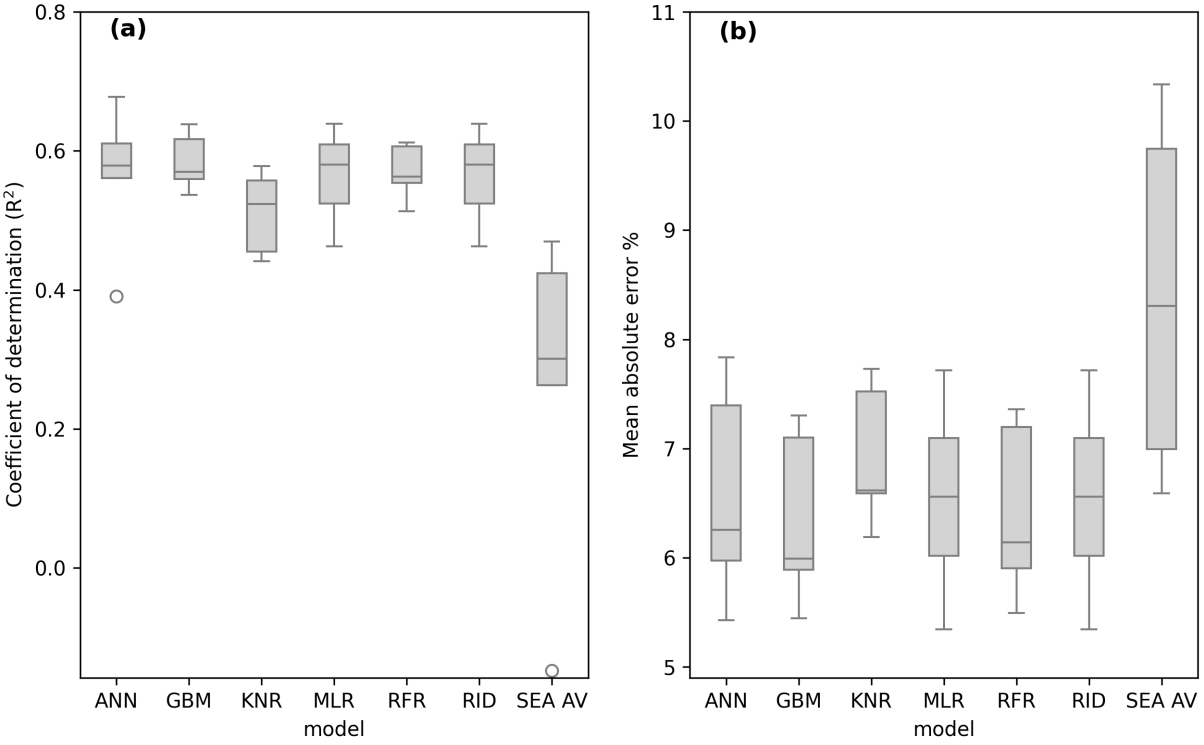

Figure 1a. VHI forecasting model performance across the hold out evaluation data set for each of the initially selected models. Results shown are for optimized hyperparameters.

Some models achieved slightly better performance with optimization such as KNR. However, more data generally resulted in better model performance rather than optimized hyperparameters. Gradient boosting (GBM) is the best performing model regardless of hyperparameter optimization.

7 Appendix B

Across months, VHI forecasts show little difference in the distribution of mean absolute error (Figure 10). However, coefficient of determination values can differ much more between months. Panel (a) of Figure 10 shows that January, February, September and October are typically the most difficult months to predict. Because R^2 differs more than mean absolute error, this indicates

that variability is more poorly captured in these months rather than a particular overall bias relating to the mis-characterization of the seasonal cycle of VHI.

Further subsequent months after 1 month into the future were assessed to determine how model performance reduces for increased lag times. Figure 10 shows how model coefficient of determination reduces from a median of 0.69 to 0.35 then 0.16 when increasing the forecast lag time from 1 to 2 then 3 months.

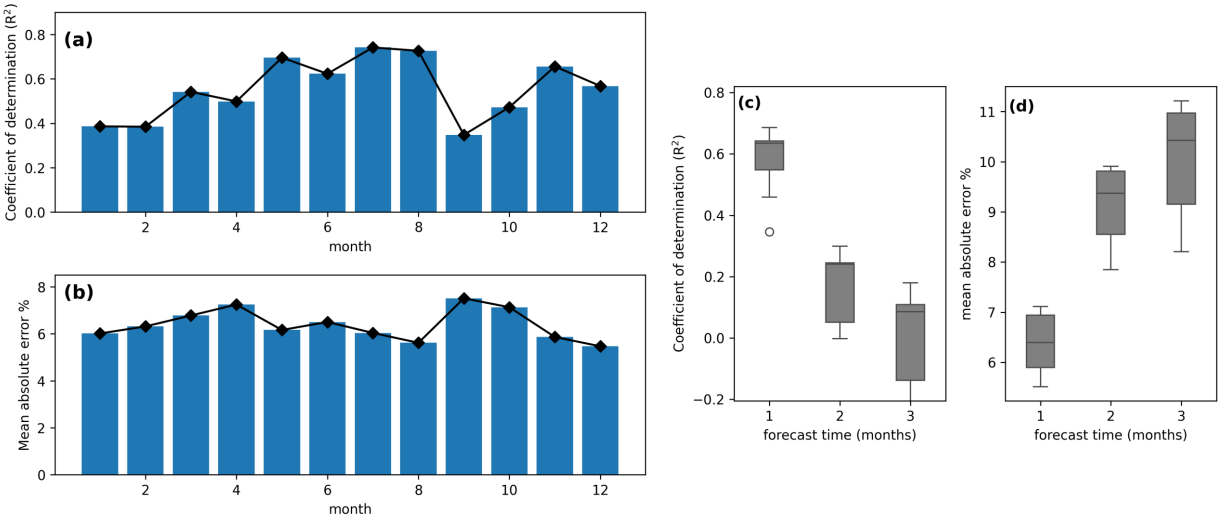

Figure 10. VHI forecasting model performance for the best model summarised as an average for each month, showing the R^2 score and mean absolute error per month (a) and (b). Secondly, model performance was compared for 2 and 3 month in advance forecasts (c) and (d).

8 Appendix C

Figure 11 shows Spearman-rank correlations between each of the input features. Highest correlations between features are between SPEI2 and 3, and SPI2 and 3 respectively, both have a Spearman-rank correlation of above 0.8. Secondly, t2m and longrad are also highly correlated (0.79).

A further variable was also included in initial tests (and in Figure 11) which was the Southern oscillation index (SOI). SOI provides an indicator of the mode of the ENSO which can show whether El Niño or La Niña conditions are likely to occur. The southern oscillation index was however shown to provide little information gain and adversely affected model performance in some instances. Therefore, this index was not included in the model results presented in this paper.

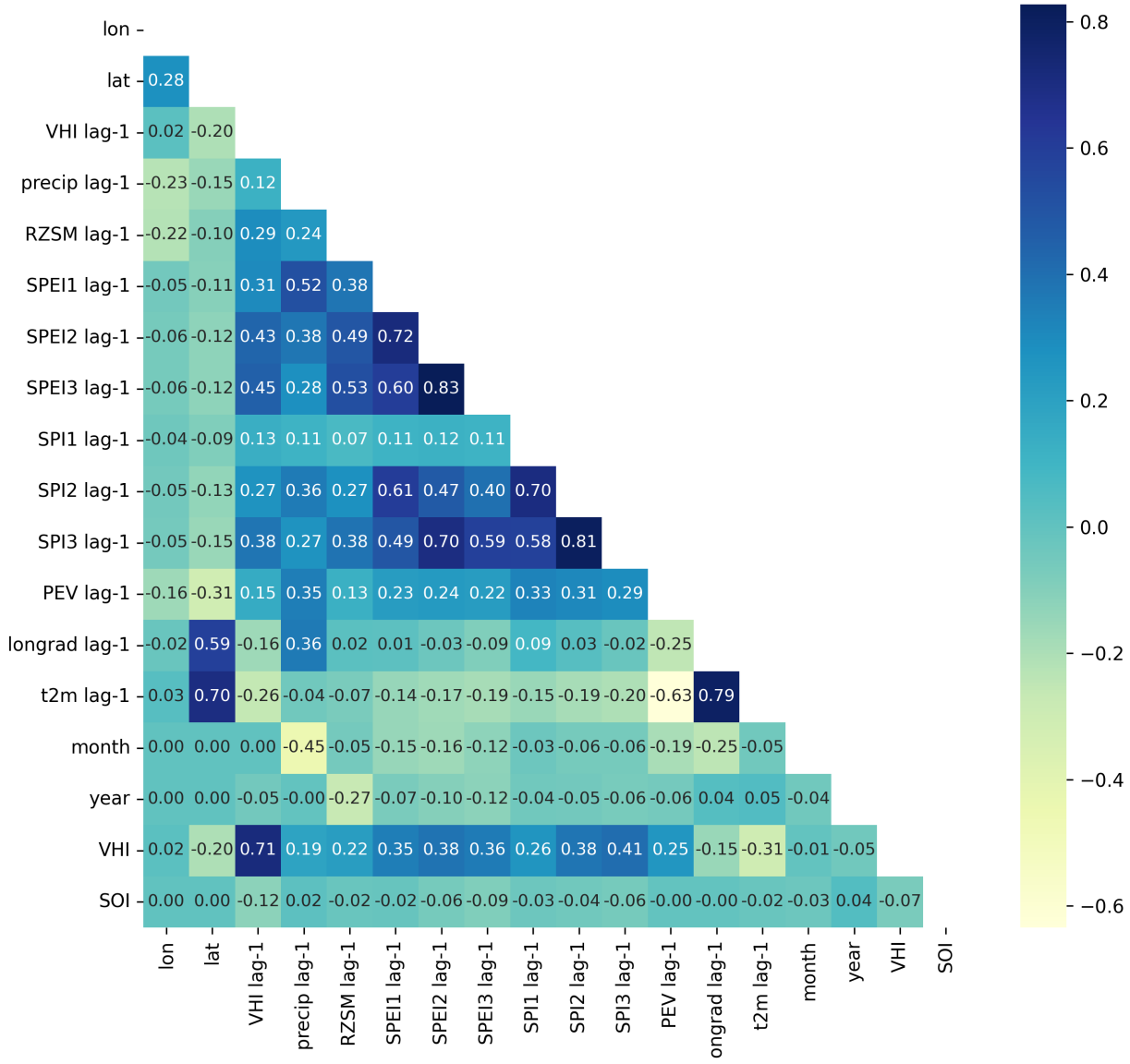

Figure 11. Spearman-rank correlation between proposed predictor variables and the target variable (VHI), lag-1 denotes a lag time of 1 month relative to time step of VHI.

9 Code availability

Code is available upon request of the corresponding author.

10 Author contribution

Joseph William Gallear wrote the text, developed the code and Figures and generated the ideas for the methods, Marcelo Zeri wrote some of the text for the introduction, methods and discussion, provided data, generated ideas for the methodological process, and provided feedback on preliminary results and discussion. Marcelo Valadares Galdos generated ideas for the methodology and provided feedback on the text of the paper and preliminary results and discussion. Andrew Hartley generated ideas for the methodology and provided feedback on preliminary results and discussion.

11 competing interests

The authors declare that they have no conflict of interest.

12 Acknowledgements

This work and its contributors (Joseph W Gallear, Marcelo Valadares Galdos, Marcelo Zeri, Andrew Hartley) were funded by the Met Office Climate Science for Service Partnership (CSSP) Brazil project which is supported by the Department for Science, Innovation & Technology (DSIT).

References

Adede, C., Oboko, R., Wagacha, P. W., and Atzberger, C.: A mixed model approach to vegetation condition prediction using artificial neural networks (ANN): case of Kenya's operational drought monitoring, Remote Sensing, 11, 1099, 2019.

agência Brasil: Drought was one of the villains of inflation in 2014, https://agenciabrasil.ebc.com.br/economia/noticia/2015-01/seca-foi-um-dos-viloes-da-inflacao-em-2014, accessed: 13/8/2024, 2015.

Barrett, A. B., Duivenvoorden, S., Salakpi, E. E., Muthoka, J. M., Mwangi, J., Oliver, S., and Rowhani, P.: Forecasting vegetation condition for drought early warning systems in pastoral communities in Kenya, Remote Sensing of Environment, 248, 111 886, 2020.

Beck, H. E., Zimmermann, N. E., McVicar, T. R., Vergopolan, N., Berg, A., and Wood, E. F.: Present and future Köppen-Geiger climate classification maps at 1-km resolution, Scientific data, 5, 1–12, 2018.

Beguería, S., Vicente Serrano, S. M., Reig-Gracia, F., and Latorre Garcés, B.: Standardized precipitation evapotranspiration index (SPEI) revisited: parameter fitting, evapotranspiration models, tools, datasets and drought monitoring, International Journal of Climatology, 34, 3001–3023, 2014.

Beguería, S., Serrano, S. M. V., Reig-Gracia, F., and Garcés, B. L.: Standardized precipitation evapotranspiration index (SPEI) revisited: parameter fitting, evapotranspiration models, tools, datasets and drought monitoring, https://doi.org/10.1002/joc.3887, 2014.

Brás, T. A., Seixas, J., Carvalhais, N., and Jägermeyr, J.: Severity of drought and heatwave crop losses tripled over the last five decades in Europe, Environmental Research Letters, 16, 065 012, 2021.

Breiman, L.: Random forests, Machine learning, 45, 5–32, 2001.

Brito, S. S. B., Cunha, A. P. M., Cunningham, C., Alvalá, R. C., Marengo, J. A., and Carvalho, M. A.: Frequency, duration and severity of drought in the Semiarid Northeast Brazil region, International Journal of Climatology, 38, 517–529, 2018.

Brodribb, T. J., Powers, J., Cochard, H., and Choat, B.: Hanging by a thread? Forests and drought, Science, 368, 261–266, 2020.

Carvalho, J. L. N., Raucci, G. S., Frazão, L. A., Cerri, C. E. P., Bernoux, M., and Cerri, C. C.: Crop-pasture rotation: a strategy to reduce soil greenhouse gas emissions in the Brazilian Cerrado, Agriculture, Ecosystems & Environment, 183, 167–175, 2014.

Chawla, N. V.: Data mining for imbalanced datasets: An overview, Data mining and knowledge discovery handbook, pp. 875–886, 2010.

Chomboon, K., Chujai, P., Teerarassamee, P., Kerdprasop, K., and Kerdprasop, N.: An empirical study of distance metrics for k-nearest neighbor algorithm, in: Proceedings of the 3rd international conference on industrial application engineering, vol. 2, 2015.

Christian, J. I., Basara, J. B., Hunt, E. D., Otkin, J. A., Furtado, J. C., Mishra, V., Xiao, X., and Randall, R. M.: Global distribution, trends, and drivers of flash drought occurrence, Nature communications, 12, 6330, 2021.

Cirino, P. H., Féres, J. G., Braga, M. J., and Reis, E.: Assessing the impacts of ENSO-related weather effects on the Brazilian agriculture, Procedia Economics and Finance, 24, 146–155, 2015.

CNA: Losses due to drought represent 7.36% of the state's GDP, says Farsul, https://www.cnabrasil.org.br/noticias/prejuizos-com-a-seca-representam-7-36-do-pib-do-estado-aponta-farsul, accessed: 13/8/2024, 2020.

CONAB: Companhia Nacional de Abastecimento, Calendario plantio e colheita, JUN 2022, https://www.conab.gov.br/, accessed:24/10/23, 2022.

Cunha, A. P. M., Zeri, M., Deusdará Leal, K., Costa, L., Cuartas, L. A., Marengo, J. A., Tomasella, J., Vieira, R. M., Barbosa, A. A., Cunningham, C., et al.: Extreme drought events over Brazil from 2011 to 2019, Atmosphere, 10, 642, 2019.

dos Santos Canalli, L. B., da Costa, G. V., Volsi, B., Leocádio, A. L. M., Neves, C. S. V. J., and Telles, T. S.: Production and profitability of crop rotation systems in southern Brazil, Semina: Ciências Agrárias, 41, 2541–2554, 2020.

Friedman, J. H.: Greedy function approximation: a gradient boosting machine, Annals of statistics, pp. 1189–1232, 2001.

Funk, C., Peterson, P., Landsfeld, M., Pedreros, D., Verdin, J., Shukla, S., Husak, G., Rowland, J., Harrison, L., Hoell, A., et al.: The climate hazards infrared precipitation with stations—a new environmental record for monitoring extremes, Scientific data, 2, 1–21, 2015.

Gidey, E., Dikinya, O., Sebego, R., Segosebe, E., and Zenebe, A.: Analysis of the long-term agricultural drought onset, cessation, duration, frequency, severity and spatial extent using Vegetation Health Index (VHI) in Raya and its environs, Northern Ethiopia, Environmental Systems Research, 7, 1–18, 2018.

Hersbach, H., Bell, B., Berrisford, P., Biavati, G., Horányi, A., Muñoz Sabater, J., Nicolas, J., Peubey, C., Radu, R., Rozum, I., et al.: ERA5 monthly averaged data on single levels from 1979 to present, Copernicus Climate Change Service (C3S) Climate Data Store (CDS), 10, 252–266, 2019.

Herweijer, C. and Seager, R.: The global footprint of persistent extra-tropical drought in the instrumental era, International Journal of Climatology: A Journal of the Royal Meteorological Society, 28, 1761–1774, 2008.

Ioris, A. A. R., Irigaray, C. T., and Girard, P.: Institutional responses to climate change: opportunities and barriers for adaptation in the Pantanal and the Upper Paraguay River Basin, Climatic change, 127, 139–151, 2014.

Júnior, R. d. S. N., Fraisse, C. W., Karrei, M. A. Z., Cerbaro, V. A., and Perondi, D.: Effects of the El Niño Southern Oscillation phenomenon and sowing dates on soybean yield and on the occurrence of extreme weather events in southern Brazil, Agricultural and Forest Meteorology, 290, 108 038, 2020.

Kartal, S., Iban, M. C., and Sekertekin, A.: Next-level vegetation health index forecasting: A ConvLSTM study using MODIS Time Series, Environmental Science and Pollution Research, pp. 1–17, 2024.

Kladny, K.-R., Milanta, M., Mraz, O., Hufkens, K., and Stocker, B. D.: Enhanced prediction of vegetation responses to extreme drought using deep learning and Earth observation data, Ecological Informatics, p. 102474, 2024.

Kloos, S., Yuan, Y., Castelli, M., and Menzel, A.: Agricultural drought detection with MODIS based vegetation health indices in southeast Germany, Remote Sensing, 13, 3907, 2021.

Kogan, F.: World droughts in the new millennium from AVHRR-based vegetation health indices, Eos, Transactions American Geophysical Union, 83, 557–563, 2002.

Kogan, F., Adamenko, T., and Guo, W.: Global and regional drought dynamics in the climate warming era, Remote Sensing Letters, 4, 364–372, 2013.

Kogan, F. N.: Global drought watch from space, Bulletin of the American Meteorological Society, 78, 621–636, 1997.

LeCun, Y., Bengio, Y., and Hinton, G.: Deep learning, nature, 521, 436–444, 2015.

Lees, T., Tseng, G., Atzberger, C., Reece, S., and Dadson, S.: Deep learning for vegetation health forecasting: a case study in Kenya, Remote Sensing, 14, 698, 2022.

Leng, G. and Hall, J. W.: Predicting spatial and temporal variability in crop yields: an inter-comparison of machine learning, regression and process-based models, Environmental research letters: ERL [Web site], 15, 044 027, 2020.

Li, B., Rodell, M., Kumar, S., Beaudoing, H. K., Getirana, A., Zaitchik, B. F., de Goncalves, L. G., Cossetin, C., Bhanja, S., Mukherjee, A., Tian, S., Tangdamrongsub, N., Long, D., Nanteza, J., Lee, J., Policelli, F., Goni, I. B., Daira, D., Bila, M., de Lannoy, G., Mocko, D., Steele-Dunne, S. C., Save, H., and Bettadpur, S.: Global GRACE Data Assimilation for Groundwater and Drought Monitoring: Advances and Challenges, Water Resources Research, 55, 7564–7586, https://doi.org/10.1029/2018WR024618, 2019.

Lopes Ribeiro, F., Guevara, M., Vázquez-Lule, A., Cunha, A. P., Zeri, M., and Vargas, R.: The impact of drought on soil moisture trends across Brazilian biomes, Natural Hazards and Earth System Sciences, 21, 879–892, 2021.

Marengo, J. A., Torres, R. R., and Alves, L. M.: Drought in Northeast Brazil—past, present, and future, Theoretical and Applied Climatology, 129, 1189–1200, 2017.

Marengo, J. A., Galdos, M. V., Challinor, A., Cunha, A. P., Marin, F. R., Vianna, M. d. S., Alvala, R. C., Alves, L. M., Moraes, O. L., and Bender, F.: Drought in Northeast Brazil: A review of agricultural and policy adaptation options for food security, Climate Resilience and Sustainability, 1, e17, 2022.

McKee, T. B., Doesken, N. J., Kleist, J., et al.: The relationship of drought frequency and duration to time scales, in: Proceedings of the 8th Conference on Applied Climatology, vol. 17, pp. 179–183, California, 1993.

Miller, L., Zhu, L., Yebra, M., Rüdiger, C., and Webb, G. I.: Projecting live fuel moisture content via deep learning, International Journal of Wildland Fire, 32, 709–727, 2023.

Nay, J., Burchfield, E., and Gilligan, J.: A machine-learning approach to forecasting remotely sensed vegetation health, International journal of remote sensing, 39, 1800–1816, 2018.

Overbeck, G. E., Vélez-Martin, E., Scarano, F. R., Lewinsohn, T. M., Fonseca, C. R., Meyer, S. T., Müller, S. C., Ceotto, P., Dadalt, L., Durigan, G., et al.: Conservation in Brazil needs to include non-forest ecosystems, Diversity and distributions, 21, 1455–1460, 2015.

Peel, M. C., Finlayson, B. L., and McMahon, T. A.: Updated world map of the Köppen-Geiger climate classification, Hydrology and earth system sciences, 11, 1633–1644, 2007.

Rebetez, M., Mayer, H., Dupont, O., Schindler, D., Gartner, K., Kropp, J. P., and Menzel, A.: Heat and drought 2003 in Europe: a climate synthesis, Annals of Forest Science, 63, 569–577, 2006.

Reddy, D. S. and Prasad, P. R. C.: Prediction of vegetation dynamics using NDVI time series data and LSTM, Modeling Earth Systems and Environment, 4, 409–419, 2018.

Rossato, L., Alvala, R. C. D. S., Marengo, J. A., Zeri, M., Cunha, A. P. d. A., Pires, L. B., and Barbosa, H. A.: Impact of soil moisture on crop yields over Brazilian semiarid, Frontiers in Environmental Science, 5, 73, 2017.

Sacks, W. J., Deryng, D., Foley, J. A., and Ramankutty, N.: Crop planting dates: an analysis of global patterns, Global ecology and biogeography, 19, 607–620, 2010.

Sadiq, M. A., Sarkar, S. K., and Raisa, S. S.: Meteorological drought assessment in northern Bangladesh: A machine learning-based approach considering remote sensing indices, Ecological Indicators, 157, 111 233, 2023.

Sena, A., Barcellos, C., Freitas, C., and Corvalan, C.: Managing the health impacts of drought in Brazil, International journal of environmental research and public health, 11, 10 737–10 751, 2014.

Sepulcre-Canto, G., Horion, S., Singleton, A., Carrao, H., and Vogt, J.: Development of a Combined Drought Indicator to detect agricultural drought in Europe, Natural Hazards and Earth System Sciences, 12, 3519–3531, 2012.

Tang, F. H. M., Nguyen, T. H., Conchedda, G., Casse, L., Tubiello, F. N., and Maggi, F.: CROPGRIDS: A global geo-referenced dataset of 173 crops circa 2020, Earth System Science Data Discussions, 2023, 1–22, https://doi.org/10.5194/essd-2023-130, 2023.

Tanguy, M., Eastman, M., Magee, E., Barker, L. J., Chitson, T., Ekkawatpanit, C., Goodwin, D., Hannaford, J., Holman, I., Pardthaisong, L., et al.: Indicator-to-impact links to help improve agricultural drought preparedness in Thailand, EGUsphere, 2023, 1–33, 2023.

Tomasella, J., Cunha, A. P. M., Simões, P. A., and Zeri, M.: Assessment of trends, variability and impacts of droughts across Brazil over the period 1980–2019, Natural Hazards, 116, 2173–2190, 2023.

Van Loon, A. F.: Hydrological drought explained, Wiley Interdisciplinary Reviews: Water, 2, 359–392, 2015.

Vicente-Serrano, S. M., Beguería, S., and López-Moreno, J. I.: A multiscalar drought index sensitive to global warming: the standardized precipitation evapotranspiration index, Journal of climate, 23, 1696–1718, 2010.

Wei, W., Wang, J., Ma, L., Wang, X., Xie, B., Zhou, J., and Zhang, H.: Global Drought-Wetness Conditions Monitoring Based on Multi-Source Remote Sensing Data, Land, 13, 95, 2024.

West, H., Quinn, N., and Horswell, M.: Remote sensing for drought monitoring & impact assessment: Progress, past challenges and future opportunities, Remote Sensing of Environment, 232, 111 291, 2019.

Wilhelmi, O. V. and Wilhite, D. A.: Assessing vulnerability to agricultural drought: a Nebraska case study, Natural Hazards, 25, 37–58, 2002.

Wu, B., Ma, Z., and Yan, N.: Agricultural drought mitigating indices derived from the changes in drought characteristics, Remote sensing of environment, 244, 111 813, 2020.

Zeri, M., S. Alvalá, R. C., Carneiro, R., Cunha-Zeri, G., Costa, J. M., Rossato Spatafora, L., Urbano, D., Vall-Llossera, M., and Marengo, J.: Tools for communicating agricultural drought over the Brazilian Semiarid using the soil moisture index, Water, 10, 1421, 2018.

Zeri, M., Williams, K., Cunha, A. P. M. A., Cunha-Zeri, G., Vianna, M. S., Blyth, E. M., Marthews, T. R., Hayman, G. D., Costa, J. M., Marengo, J. A., Alvalá, R. C. S., Moraes, O. L. L., and Galdos, M. V.: Importance of including soil moisture in drought monitoring over the Brazilian semiarid region: An evaluation using the JULES model, in situ observations, and remote sensing, Climate Resilience and Sustainability, 1, https://doi.org/10.1002/cli2.7, 2022.

Ziese, M., Becker, A., Finger, P., Meyer-Christoffer, A., Rudolf, B., and Schneider, U.: GPCC First Guess Product at 1.0: Near real-time first guess monthly land-surface precipitation from rain-gauges based on SYNOP data, 2011.